PORE PRESSURE EFFECTS AND PERMEABILITY: EFFECTIVE STRESS ISSUES FOR HIGH PRESSURE RESERVOIRS

Greg Boitnott, *New England Research, Inc.*
Terry Miller, *Geomechanics and Testing Analysis*
John Shafer, *Consultant*

This paper was prepared for presentation at the International Symposium of the Society of Core Analysts held in Noordwijk, The Netherlands 27-30 September, 2009

ABSTRACT

Rock properties models for the deep water Lower Tertiary sandstones from the Gulf of Mexico need better calibration for conditions of high initial pore pressures and large pore pressure depletions. Available data indicates that inelastic pore compaction at high drawdowns is possible and significant permeability reduction may occur due to both elastic and inelastic deformations. Even in the elastic regime, anomalous pore pressure effects on key reservoir properties have been observed.

Core measurements used to calibrate logs, interpret seismic data, and constrain reservoir simulations are commonly made at low pore pressures. To mimic reservoir conditions, the tests are commonly performed at reduced external stresses (σ), so as to compensate for the low pore pressures (P_p) used in rock testing. We show that due to a variety of pore pressure phenomena, laboratory measurement of brine permeability indicate that for these Lower Tertiary sandstones, the routine core permeability measurements at low pore pressure may underestimate the in-situ rock permeability and underestimate permeability reduction due to depletion. Permeability measurements collected during multiple cycle stress paths are presented. We demonstrate how the data are used for evaluating effective stress coefficient for permeability and discuss issues with the concept of effective stress when applied to reservoir engineering problems.

INTRODUCTION

An effective stress law is a means to convert two variables, external stress (σ) and pore pressure (P_p), into one equivalent variable ($\sigma_{effective}$). One such expression would be $\sigma_{effective} = \sigma - \boldsymbol{a}\, P_p$, where $\boldsymbol{a}$ is the "effective stress coefficient". Every rock property; e.g. permeability, compressibility, and acoustic velocities, has its own effective stress coefficient (see Robin, 1973, and Berryman, 1993). This coefficient is found to be less than 1.0 for many rock properties, is commonly thought to be 1.0 for strength and static elastic constants, and can be greater than 1.0 for permeability (e.g. Al-Wardy and Zimmerman, 2004).

The effective stress coefficient for bulk volume compressibility, the Biot Coefficient α, is probably the most recognized effective stress coefficient. The Biot Coefficient is well understood in terms of poroelasticity, and experimental data on reservoir sandstones

typically fit theory very well. Simple poroelasticity leads to the now familiar effective stress law for hydrostatic volume compressibility, equation (1).

$$\varepsilon_v = P_e / K_b \quad ; \quad P_e = P_c - \alpha P_p \quad ; \quad \alpha = 1 - K_b/K_g \qquad (1)$$

where ε_v is the volumetric strain, P_c is the confining pressure, P_e is the effective pressure, K_b is the bulk modulus of the rock, and K_g is the bulk modulus of the solid grains. The temptation is to assume that the "effective pressure" P_e defines an equivalent state of stress that, when applied to a rock in the absence of pore pressure, results in an equivalent physical state (thus removing pore pressure as a variable). In fact however, P_e as defined in equation 1 is little more than a functional relationship between P_c and P_p that yields identical bulk volume for the case of an isotropic, linear elastic, porous solid. Often we find that it is substituted for the effective stress coefficient in effective stress relations for other rock properties, or used to establish stress conditions for petrophysical or geomechanical tests. We will show that in many cases this may not be appropriate, and can lead to potentially erroneous estimates of reservoir properties.

One example is the case of permeability. Experimental evidence suggests that for many sandstones, the effective pressure coefficient for permeability (α_k) can be significantly greater than 1 (Zoback, 1975; Zoback and Byerlee, 1975, Walls and Nur, 1979, Warpinski & Teufel, 1992, Al-Wardy and Zimmerman, 2004), while α for bulk volume is less than or near 1. In these studies, a variety of porous sandstones with porosities in the range 16 – 24 percent and clay contents of 5 – 20 percent where found to exhibit α_k near 2 or higher. In such cases, the permeability is observed to increase with increasing pore pressure at a constant net confining stress. Simple poroelasticity arguments however predict that the opposite should occur, e.g. that the effective stress coefficient for permeability should be slightly less than 1 (Bernabe et al., 1982; Zimmerman, 1991, Al-Wardy and Zimmerman, 2004). The rational for the observed "anomalous" effect of pore pressure is that in addition to simple poroelastic deformation of the load bearing frame, pore pressure acts to deform grains that are isolated from the external stresses (e.g. pore lining clays). This deformation of pore filling minerals effectively changes the diameter of the pores and throats and thereby the permeability. Others have questioned both the proposed mechanism and potentially the result. Based on a set of experiments on Berea Sandstone, Coyner (1984) postulated that residual hydrocarbons, rather than clays, may be the cause of the $\alpha_k>1$.

In a recent paper, Shafer et al. (2008) reported a values of α_k = 2.58, 2.48, and 1.16 for three extracted reservoir sandstones from the Lower Tertiary Gulf of Mexico. In that work, Shafer et al. discuss some potential issues related to loading protocol and suggest a specific protocol involving a particular sequence of different pressure changes to assure that the results are not contaminated by stress history dependence and other inelastic effects. Shafer et al. also discuss the case of non-hydrostatic stresses, illustrating potential biases due to systematic differences in loading path when a uniaxial strain compaction test at constant pore pressure is used to simulate pore pressure depletion.

Here we report on additional experiments designed to address these questions of loading protocol and loading path. New experimental results using a sandstone from a Lower Tertiary Gulf of Mexico discovery provide additional support for the observation that

α_k>1 for porous sandstones containing intra-pore clay. Loading hysteresis effects are illustrated, and for the conditions tested are found to gradually reduce in magnitude with repeated cycling. It is shown that for the Lower Tertiary sandstone sample studied, loading path differences in the case of uniaxial strain pressure depletion lead to significantly different estimates of permeability reduction due to drawdown.

EXPERIMENTAL RESULTS

System Description

A schematic illustration of the apparatus used in this work is shown in Figure 1. The samples were vacuum saturated with brine, jacketed in Viton sleeves, and mounted between grooved end caps. The axial stress, confining pressure (mineral oil) and the two pore pressure intensifiers (brine) were hydraulically servo-controlled. For hydrostatic testing protocols, the axial stress intensifier and platten were removed from the system such that the confining pressure exerted a hydrostatic stress on the sample. Computer control software was used to run each experiment, and the equipment and protocol were designed such that the experiment could be fully automated with no interruption or operator intervention. Changes in stress were continuous and simultaneous.

Permeabilities were measured using a low volume steady-state flow technique. Prior to each permeability measurement, all stresses and pressures where held constant so that the system was in static equilibrium. Each measurement involved establishing a 1 MPa pressure difference between the two pore pressure intensifiers and flowing 7cc of simulated reservoir brine through the sample. Flow rate and pressure difference were monitored continuously and permeability was computed based on the average flow rate and pressure gradient over a time window between 1cc and 6cc volume net flow. At the conclusion of each permeability measurement, the pressures were ramped to the next measurement condition while simultaneously re-stroking the pore pressure intensifiers (i.e. net flow back through the sample) to get ready for the next measurement. Once at the new stress and pressure conditions, the next permeability measurement sequence was initiated.

Protocol

We begin by considering the case of hydrostatic external stresses (e.g. $\sigma_{axial} = \sigma_{radial} = P_c$). In order to determine an effective stress coefficient for a given property (e.g. permeability, k), that property is measured at various combinations of stress and pore pressure. The results are then fit to a functional relation $\boldsymbol{f}(\ )$ involving the effective stress [e.g. $k = \boldsymbol{f}(P_c - \alpha_k P_p]$, where α_k is the effective stress coefficient for the property k. The effective stress coefficient is determined by finding the best fitting value of α_k.

There are three basic sets of confining and pore pressure changes (referred to here as loading paths) typically used to study effective stress:

1) simultaneous and equal changes in confining and pore pressure;
2) changes in pore pressure at constant confining pressure; and
3) changes in confining pressure at constant pore pressure.

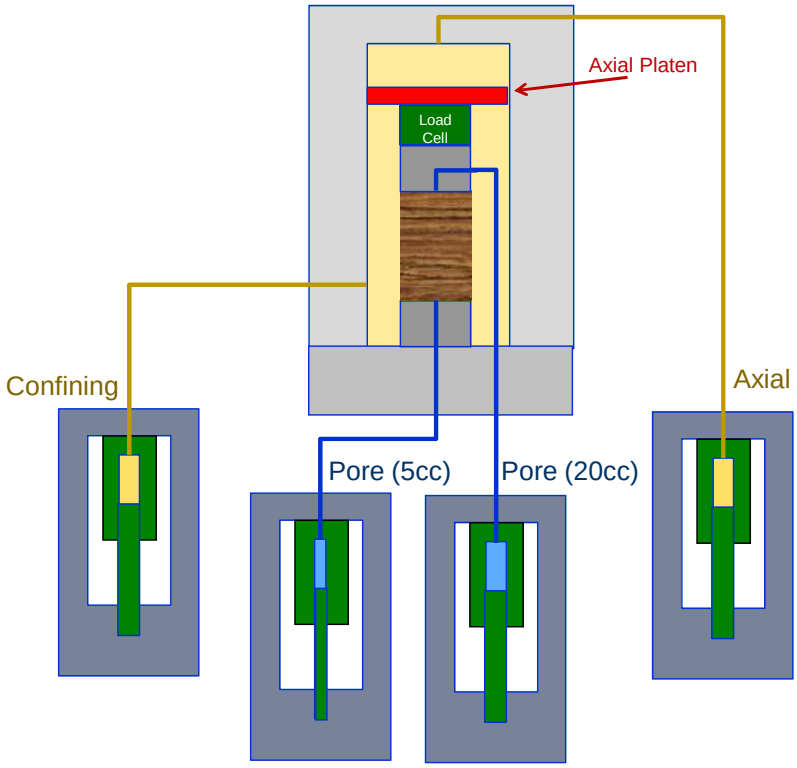

Figure 1: Schematic diagram of the testing apparatus. Four hydraulic intensifiers provide independent control of the axial stress, confining pressure, and upstream and downstream pore pressures. The axial platen and axial intensifier are removed for tests involving hydrostatic confining and pore pressure only.

For the simple case of a sample that deforms elastically with no hysteresis in permeability, measurements of the change in permeability using a combination of any two of these loading paths is sufficient to infer α_k . Historically most measurements of α_k have been made using a combination of loading paths 2 and 3, and various protocols and data analysis methods have been used. One concern that is always difficult to address is the potential impact of time and stress history dependence. These issues are common in permeability testing due to sensitivity of permeability to inelastic deformation as well as due to issues such as fines migration. As a result, it can be difficult to be sure that inferences of α_k are not biased by choice of loading protocol. Another common and related issue is that the stress and pressure dependence of permeability in many reservoir sandstones is typically small, and thus α_k is commonly determined by the ratio of two small values, each with their own systematic errors. It is thus helpful to design a protocol that incorporates repeated cycles and makes use of all three loading paths in order to have some redundancy. Protocols should check explicitly for the requirement that in order for α_k to have meaning, permeability must be a unique (uni-valued) function of P_c and P_p, regardless of the loading path or history.

An example stress history used in this study is shown in Figure 2. The protocol consists of multiple cycles of all three types of loading (e.g. 1, 2, and 3 listed above). In principle, α_k can be inferred from the changes in permeability due to any two of these loading segments based on the following relationships:

$$\alpha_{k12} = [\ 1 - (\partial k/\partial P_p)|_{Pd} / (\partial k/\partial P_p)|_{Pc}\ ]^{-1} \quad (2a)$$
$$\alpha_{k13} = 1 - (\partial k/\partial P_p)|_{Pd} / (\partial k/\partial P_c)|_{Pp} \quad (2b)$$
$$\alpha_{k23} = -(\partial k/\partial P_p)|_{Pc} / (\partial k/\partial P_c)|_{Pp} \quad (2c)$$

Where $P_d=P_c-P_p$, α_{k12} refers to a measurement of α_k using loading paths 1 and 2, α_{k13} refers to a measurement of α_k using loading paths 1 and 3, and α_{k23} refers to a measurement of α_k using loading paths 2 and 3.

As recommended by Shafer et al. (2008), we feel that it is preferable to begin with load path 1, since path 1 is least likely to cause any permanent deformation of the sample and can be designed to end with the sample at *in situ* conditions. We follow path 1 cycling with cycling of path 2, which is preferred over path 3 because it more closely represents what happens in the reservoir during depletion. We then follow with path 3 cycling for redundancy in the determination of α_k. The addition of load path 3 is also important in that pore pressure is held constant, thus removing (from this portion of the test) the effects of pore pressure on viscosity that must be applied to load paths 1 and 2 in the computation of permeability.

In the experiments presented in this work, we performed all permeability testing using brine as the pore fluid at ambient temperature (140g/l NaCl with minor KCL and CaCl2). Over a wide range of compositions, brine (and water) has the unique property that the pressure dependence of viscosity has a minimum near room temperature (Phillips et al., 1981). Over the pressure ranges involved here, the pressure dependence of viscosity is considered to vary by less than 1%, and thus pressure dependence is neglected in our analysis. If these tests had been performed at elevated temperatures, or using a pore fluid other than brine or water, uncertainty in the pressure dependence of viscosity would be of considerable concern.

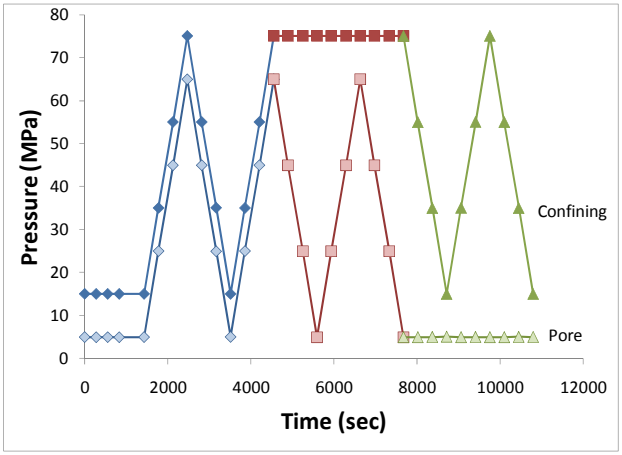

Figure 2: Time history of a hydrostatic effective pressure experiment. The test sequence involves coordinated changes in hydrostatic confining and pore pressures in a sequence of three different loading paths: (1) ♦ simultaneous and equal changes in confining and pore pressure (constant net confining stress); (2) ■ changes in pore pressure at constant confining pressure; (3) ▲ changes in confining pressure at constant pore pressure. Symbols indicate points at which permeability is measured.

Hydrostatic Test Results

The results from an experiment on a Lower Tertiary reservoir sandstone for the Gulf of Mexico are shown in Figure 3. The sandstone had an initial permeability of 15mD and porosity of 20 percent. Plots of normalized permeability (k_n) versus P_c, P_p, and P_c-P_p are provided. Normalized permeability is the measured permeability divided by the permeability at the start of the test. In general we find the pressure dependence of permeability to be approximately linear over the range of pressures tested. Quick inspection of the data indicates $\alpha_k>1$, as we observe permeability increasing with increasing P_p at constant P_c-P_p (e.g. blue diamonds in the right plot in Figure 3). This indicates that P_p has a larger effect on permeability than does P_c. It is also clear from the plot of permeability versus P_c-P_p that the pressure dependence of permeability for loading path 2 is notably larger than that of loading path 3. This again indicates that pore pressure has a larger effect on permeability than does the confining pressure[1].

Fitting slopes to the various loading path data and using equations 2a-c, we find α_{k12}=2.0, α_{k13}=2.4, and α_{k23}=2.8. In fitting the slopes however, we had to ignore the first half cycle of loading path 2. This loading leg was the samples first excursion to high P_c-P_p and is thus the first time in the test that grain contact stresses where increased to high level. As is common in rock testing, this first loading (even in the elastic regime) results in a permanent set in the permeability (i.e. a non-elastic response). It should be noted that had we not done multiple cycles of loading path 2, we would have inferred a larger value of $(\partial k/\partial P_p)|_{Pc}$ which would have lead to a lower a_{k12} and a higher α_{k23} – thus increasing the discrepancy between estimates of α_k.

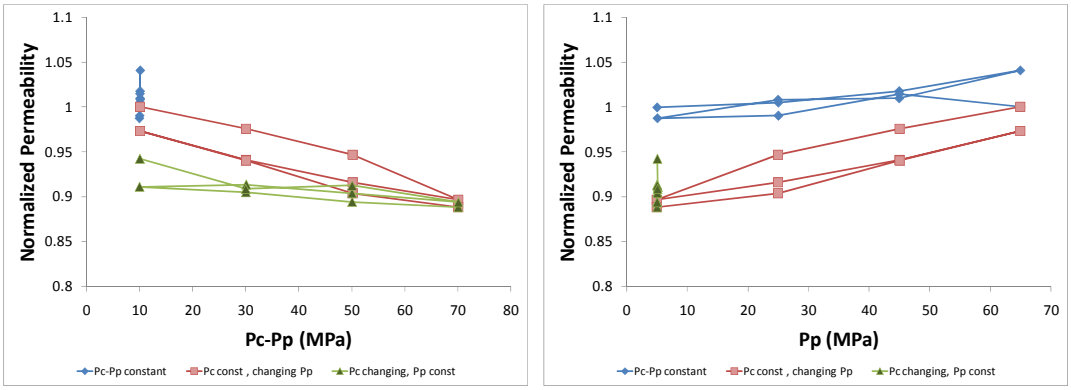

Figure 3: Results of the first hydrostatic test on a reservoir sandstone using the loading protocol shown in Figure 2. The pressure dependence of permeability is found to be approximately linear for each loading path over the range of pressures tested. The first loading leg of loading path 2 resulted in a non-recoverable loss in permeability of about 5%. The last data point from loading path 1 also indicates a permanent loss in permeability, the cause of which is unknown. Results from the rest of the experiment indicate a weak but reproducible pressure dependence of permeability.

[1] We note that the magnitude of the measured changes in permeability for this sample are less than the minimum standard industry error for permeability (±5%) for sandstones in this permeability range. The trends used here and throughout are considered significant in that the variation defining the trends does not appear random.

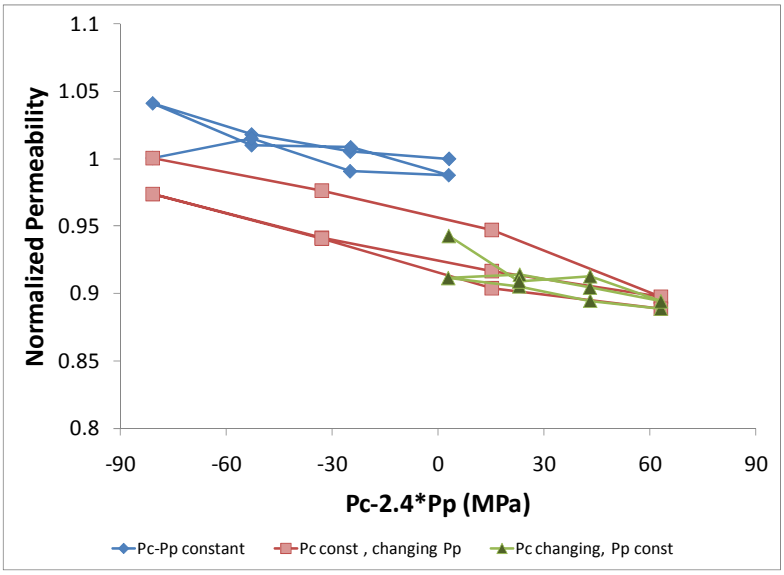

Figure 4: A plot of normalized permeability versus Pc-2.4Pp for the data in Figure 3. Using this average value of α_k, the data from the three loading paths, fall on a common slope, indicating consistency with an effective stress coefficient of α_k=2.4. The progressive loss in permeability throughout the experiment, mostly due to the first excursion to elevated Pd=Pc-Pp (■) is easily seem in this view. This results from a combination of stress and time dependence in the permeability, probably resulting from inelastic deformation with stress cycling and possibly also some progressive changes in permeability with fines migration.

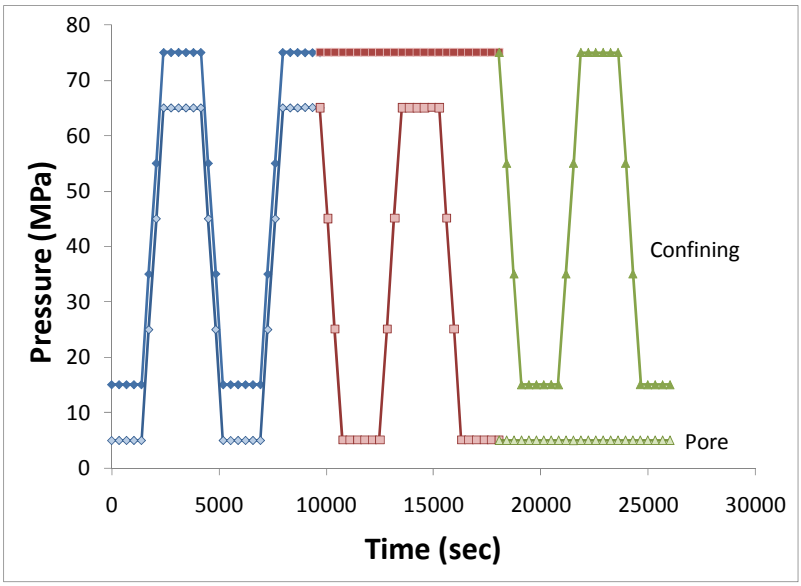

Figure 5: A revised protocol designed to better constrain any stress history and/or time dependence if present. Symbols indicate points at which permeability was measured during each of the three different loading paths: (1) ♦ simultaneous and equal changes in confining and pore pressure (constant net confining stress); (2) ■ changes in pore pressure at constant confining pressure; (3) ▲changes in confining pressure at constant pore pressure.

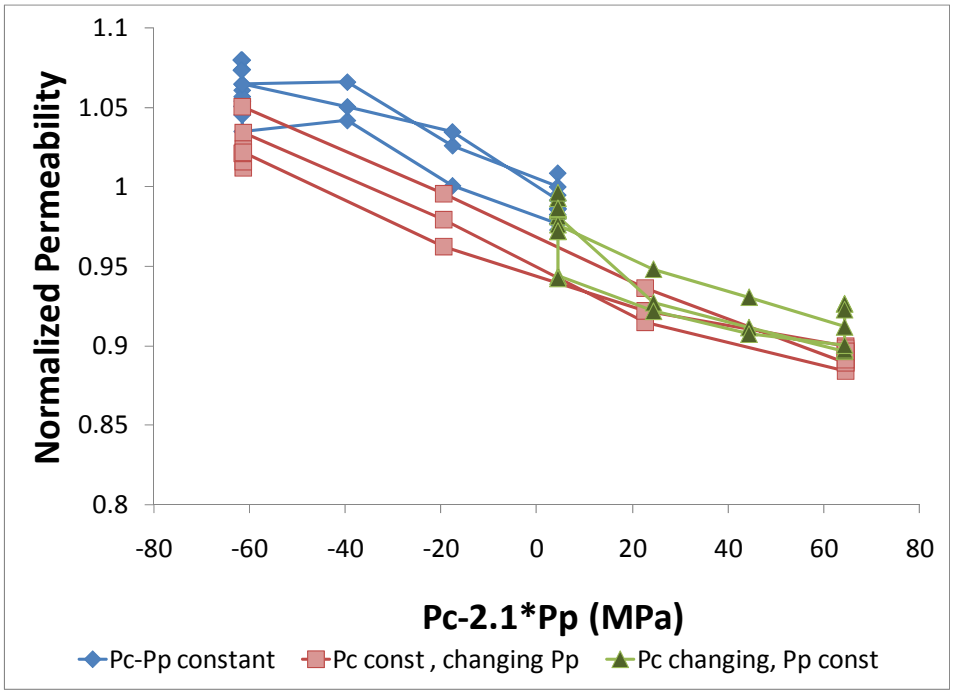

Figure 6: Result from the same sample as in Figure 4, after repeated testing and using the protocol in Figure 5. Note we infer similar α_k as in the first test (e.g. Figures 3 and 4) but with less stress history and/or time dependence and thus more internal consistency. This is thought to be the result of repeated stress cycling, conditioning the sample to a more elastic response.

Taking our average value of α_k=2.4, we produce the result shown in Figure 4. Note that excluding the first loading segment of loading path 2, the permeability vs. P_c-2.4P_p plot yields a family of parallel lines reflecting the consistency of results from the three loading paths.

To explore further the loading path history and/or time dependence of permeability, the sample was tested again multiple times without relieving stresses, each time producing a similar result but with progressively less stress history dependence. During this repeated testing that occurred over a period of 5 days, the permeability of the sample reduced gradually by 30% (note over 5% reduction was observed in the first test as shown in Figure 3). After a number of cycles, a more advanced protocol was implemented to better probe possible time and stress history dependence. The protocol is shown in Figure 5, and the results from the test are shown in Figure 6. This protocol was implemented in part to test for possible thermal effects (due to adiabatic heating of the confining and pore fluids) which might adversely affect the results. No such effects are observed in the data. Note that by this point in the testing of the sample, the stress history and time dependence had become negligible. The results from the test in Figure 6 yield α_{k12}=2.2, α_{k13}=2.1, and α_{k23}=2.0, exhibiting good internal consistency in α_k over the entire loading path.

Reservoir Depletion Test Results

While the concept of effective pressure is relatively straight forward for the case of hydrostatic loading, Shafer, et al (2008) point out for realistic stress paths during

reservoir depletion, another effect may be even more important. When pore pressure decreases in a thin tabular reservoir, it is commonly assumed that the loading path is one of uniaxial strain (e.g. the lateral strain is held constant). This leads to the condition that the lateral stress changes differently from the vertical stress.

It is commonly assumed that in rock testing, the uniaxial strain loading path at fixed pore pressure is an adequate substitute for the more difficult to perform uniaxial strain loading during pore pressure depletion. However, due to finite grain compressibility, it can easily be shown (both theoretically and experimentally) that these two loading paths lead to differences in stress conditions (Zimmerman, 2000, Shafer et al 2008). These differences can be significant when considering production scenarios of deep, high pressure reservoirs.

The protocol used in the non-hydrostatic test is shown in Figure 7. It is similar in principle to the hydrostatic protocol in Figure 5, but with the addition of axial load. The axial and confining pressures where changed following the paths predicted by poroelasticity: e.g. $\partial\sigma_r/\partial\sigma_a\,|_{Pp=const} = \nu/(1-\nu)$ and $\partial(\sigma_{re})/\partial(\sigma_{ae})|_{\sigma a=const} = 1-\alpha(1-2\nu)/(1-\nu)$, were α is the Biot coefficient from equation 1, ν is the Poisson's ratio, σ_r is the external radial stress (e.g. P_c), σ_a is the external axial stress, $\sigma_{re}=\sigma_r - P_p$, and $\sigma_{ae}=\sigma_a-P_p$. For this demonstration experiment, we assumed $\alpha=0.78$ and $\nu=0.2$ based on geomechanics testing on related samples. In practice it would be preferable to do true uniaxial strain testing as was done in Shafer et al. (2008), but for demonstration purposes, the test performed for this study was done using simple stress trajectories determined from poroelasticity.

The permeability results from this test are shown in Figure 8. Here we have plotted the permeability as a function of effective drawdown, which for the pore pressure depletion path is simply the change in pore pressure (e.g. $P_{pinitial} - P_p$) and for the constant pore pressure leg is the change in axial "effective" stress $\sigma_{ae} - \sigma_{ae\_initial}$. We note that, as postulated by Shafer et al. (2008), the two loading paths do not have an equivalent effect on permeability. The starting permeability is higher for the case of true pore pressure depletion (as a result of the $\alpha_k>1$ effect) and reduces more with drawdown. The increased permeability reduction for the case of pore pressure depletion is likely the result of both $\alpha_k>1$ and the difference in loading trajectory. Further analysis of this test can be found in Boitnott et al. (2009).

DISCUSSION

Our experimental results support the observation that for sandstones from the Lower Tertiary Gulf of Mexico play, the effect of confining and pore pressure on permeability can be described using a single effective pressure P_e defined by the relation $P_e=P_c-\alpha_k P_p$, with $\alpha_k>1$. For the reservoir sample studied here, α_k is found to be slightly greater than 2. Our results indicate that the anomalous pore pressure effect leading to $\alpha_k>1$ results from a recoverable process, consistent with models of elastic deformation of compliant pore linings isolated from external stresses.

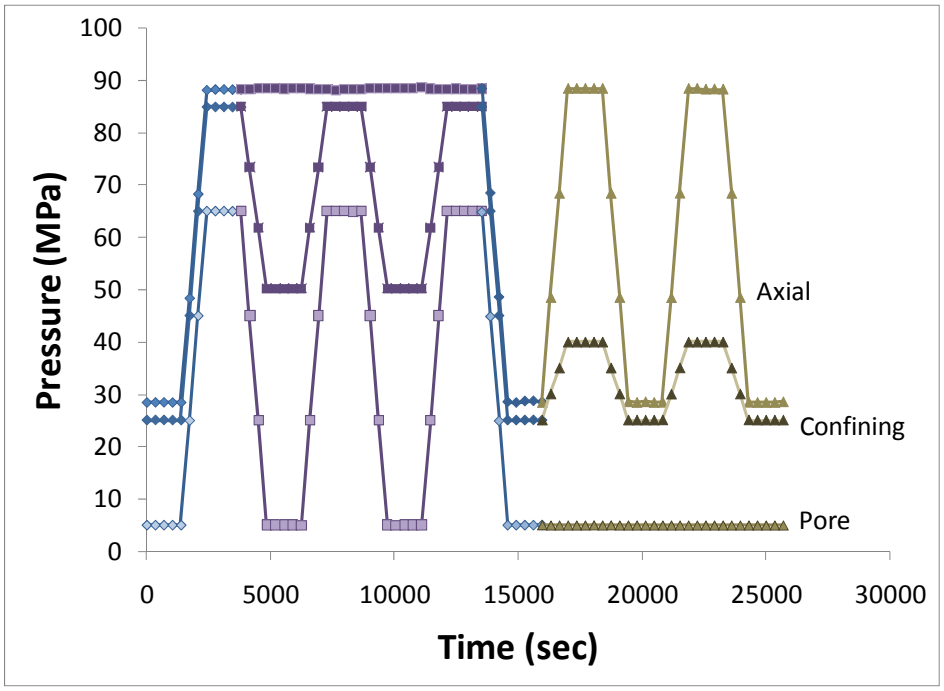

Figure 7: The loading protocol used to study the difference between true pore pressure depletion and simulated pore pressure depletion for the case of poro-elastic deformation. Symbols indicate points at which permeability was measured during each of the three different loading paths: (1) ♦ simultaneous and equal changes in stresses and pore pressure; (2) ■ pore pressure depletion at constant axial stress; (3) ▲changes in effective drawdown at constant pore pressure.

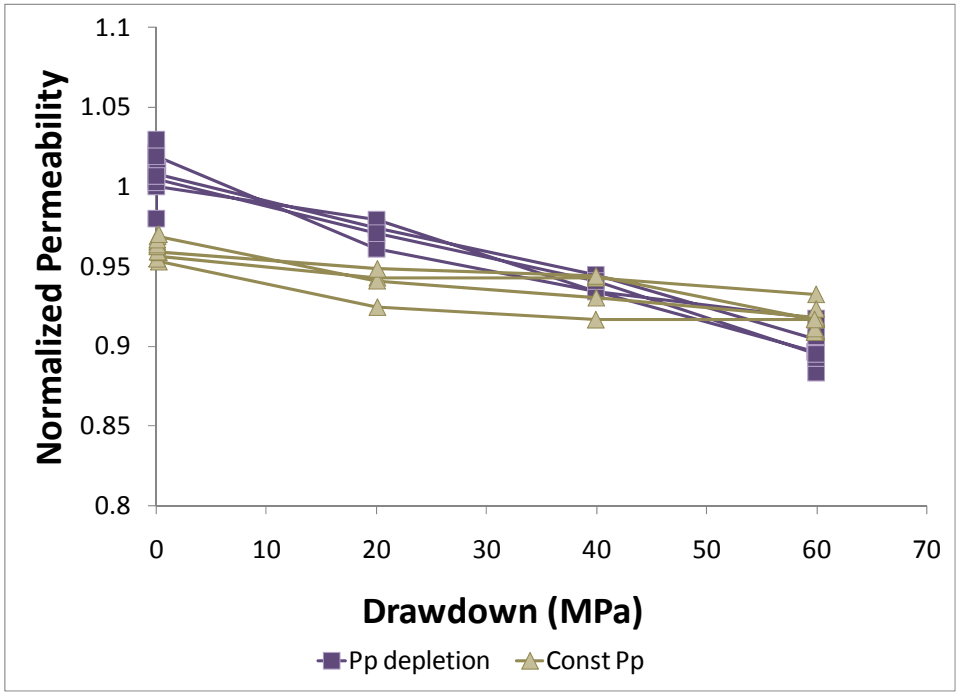

Figure 8: A plot of normalized permeability versus effective drawdown for the experiment shown in Figure 7. Note the systematic differences between the pore pressure depletion and constant pore pressure results.

Permeability tests are typically conducted in conjunction with other tests, e.g., compressibility or shear-strength studies. It is important to keep in mind that the effective stress-coefficients for these tests can be quite different. As a consequence studies conducted with reduced total stresses and pore pressures may cause unanticipated or unrealistic physical responses that would not occur at *in situ* stresses and pore pressures.

Shafer, et al (2008) briefly discuss the differences in loading paths for constant pressure vs. pressure depletion compressibility tests on stiff rocks found in some HTHP reservoirs. The two tests are both conducted under conditions of uniaxial strain in which the axial stress is varied while confining pressure is controlled to enforce zero lateral strains in the sample. These tests are assumed to best represent rock behavior *in situ*. In a pressure depletion test, the rock sample rock sample is initially subjected to the in situ pore pressure and total stresses and then the pore pressure is reduced by a planned amount. In a constant pressure test, the rock sample is initially subjected to an initial in situ effective stress condition with reduced total stresses and pore pressure and then the axial stress is increased to simulate the effects, via effective stress changes, of pressure drawdown.

Results from our test comparing permeabilities measured during pore pressure depletion and constant pore pressure uniaxial strain loading paths confirm that the pore pressure depletion test results in higher initial permeability and larger permeability reduction than the constant pore pressure test for equivalent effective drawdowns. Part of this difference likely results from the same physical mechanism that leads to $\alpha_k>1$ for the hydrostatic case. However, the two tests differ in other ways as well, most notably that they produce loading paths that follow different effective stress paths. As a result of grain compressibility effects, pore pressure depletion at constant lateral strain leads to lower P_c-P_p for a given σ_{axial}-P_p. This difference in effective stress path likely influences differences in measured permeabilities as well. Understanding the relative contributions of these two effects requires more study.

Each physical property of interest responds to external stresses and pore pressures in a different way, and thus each property will have its own effective pressure coefficient. Note that by definition, the different effective reservoir stresses are matched in a pressure depletion test since this test reproduces as closely as possible initial reservoir conditions. The differences are a result of the different coefficients for the effective stress relations that govern different properties. For example, one may decide to perform a test at low pore pressure by matching the effective stress for bulk volume (i.e. $P_c - \alpha P_p$) where α may be near 0.7, but that stress condition will not be appropriate for permeability, where α_k may be near 2.0. Other properties such as strength, which is commonly thought to be controlled by mean stress minus P_p thus requires yet another coefficient $\alpha_{strength}=1$. The combination of having stiffer rocks and very high pressures can lead to large differences in the magnitude of the various effective stresses.

Even in the elastic regime, the differences in effective stress coefficients for different properties can be significant and grain compressibility effects can lead to significantly different loading paths for what otherwise might be thought of as equivalent loading paths.. For these reasons, we conclude that whenever possible, rock testing should be performed using stresses and pore pressures representative of reservoir conditions. Use

of the concept of effective stress, while clearly useful, should not be done without careful consideration of these effects.

ACKNOWLEDGEMENTS

The authors would like to thank Jon Knut Ringen and Jules Reed for very helpful reviews of the manuscript. We thank Peter Boyd for his assistance in performing the laboratory experiments.

REFERENCES

1. Al-wardy, W. and Zimmerman, R.W., 2004, “The Effective stress law for the permeability of clay-rich sandstones”, J. of Geophy. Res., 109, B04203, 10 pages.
2. Berryman, J. G. 1993, `` Effective-stress rules for pore-fluid transport in rocks containing two minerals," Int. J. Rock Mech. Min. Sci. & Geomech. Abst. 30, 1165-1168.
3. Boitnott, G. N., Miller, T. W., and Shafer, J. L., 2009, Pore-Pressure Depletion and Effective Stress Issues in the Gulf of Mexico's Lower Tertiary Play, SPE 124790-PP, SPE Annual Technical Conference and Exhibition held in New Orleans, Louisiana, USA, 4–7 October 2009
4. Coyner, K., 1984, Effects of stress, pore pressure, and pore fluids on bulk strain, velocity, and permeability in rocks, PHD Thesis, MIT.
5. Phillips, S.L.; Igbene, A.; Fair, J.A.; Ozbek, H.; and Tavana, M., 1981, A Technical Databook for Geothermal Energy Utilization, Lawrence Berkeley Laboratory, University of California, Berkeley, CA.
6. Robin, P., 1973, “Note on Effective Pressure, Jr. of Geophysical Research, 78, n14, pp2434-2437.
7. Shafer, J., Boitnott, G., and Ewy, R., 2008, Effective Stress Laws for petrophysical rock properties, Proceedings SPWLA 49th Annual Logging Symposium.
8. Warpinski, N.R., and Teufel, L.W., 1992, “Determination of the Effective Stress Law for Permeability and Deformation in Low-Permeability Rocks,” SPE Formation Evaluation, June, 123-131.
9. Walls, J., and Nur, A., 1982, Pore pressure and confining pressure dependence of permeability in sandstone, Proceedings of the 7th Formation Evaluation Symposium of the CWLS, paper O, Canadian Well Logging Society, Alberta, Calgary.
10. Zimmerman, R., 2000, Implications of Static Poroelasticity for Reservoir Compaction, Proc. 4th North Amer. Rock Mech. Symp., A.A. Balkema, Rotterdam, pp. 169-72.
11. Zoback, M. D, 1975, High pressure deformation and fluid flow in sandstone, granite , and granular materials, PH.D. Thesis, Stanford University.
12. Zoback, M.D. and Byerlee, J. D., 1975, Permeability and effective stress, AAPG Bull. V59, 154-158.